Reprinted from ADVANCES IN CHEMISTRY SERIES, Number 133
Chemical Reaction Engineering—II




# Mathematical Modeling of the Monolith Converter

LARRY C. YOUNG and BRUCE A. FINLAYSON

Department of Chemical Engineering, University of Washington, Seattle, Wash. 98195

*Mathematical models for the monolith converter are developed and applied to the oxidation of carbon monoxide in automobile exhausts. The converter consists of an array of ducts with catalyst coating the walls. The exhaust gas flows axially through the ducts in laminar flow. Two models for this type of converter are proposed and solved numerically. The simpler model uses heat and mass transfer coefficients for fully developed flow in ducts to account for the resistance to transfer between the fluid and the catalytic wall. The more complicated model accounts for the distribution of mass and energy in the duct cross-section, which is assumed to be circular. Both transient and steady-state calculations are performed for conditions which would be expected during vehicle operation. Mass and energy distribution in the duct cross-section is important. Transient calculations predict that the wall temperature can overshoot the steady-state adiabatic temperature and thus contribute to converter failure.*

One of the contemporary challenges to technology is the control of automobile emissions. A promising method of meeting emission standards in the short term is to use catalytic converters. In this preliminary study the authors propose and solve two mathematical models for a particular type of converter, the monolith converter. Particular attention is given to the use of efficient computing techniques. Both transient and steady-state calculations are performed for conditions which could be expected in automobile operation, and the essential features of the problem are outlined.

Two types of catalytic converters, packed beds and monoliths, have been proposed for the oxidation of carbon monoxide and hydrocarbons in automobile exhausts. Mathematical models have been proposed and solved for packed bed converters (*1*, *2*, *3*, *4*) while Kuo (*5*) has developed a model for the monolith converter which is similar to the simpler one solved here.

The monolith converter consists of an array of ducts or cells through which the exhaust gas flows axially. The internal surface area of the substrate material is relatively low; therefore, a wash coat of catalyst dispersed on activated alumina is deposited on the substrate. Because of a much smaller volumetric heat capacity, monolith converters warm up more quickly than

packed bed devices, giving the monolith an important advantage during cold starts of the engine. The monoliths have difficulties, however, caused by thermal expansion, and in certain driving modes the monolith substrate can melt, resulting in converter failure (*6*). The mathematical models developed below illustrate important features of the thermal behavior of the monolith converter.

### *Model Development*

Available information on the reaction kinetics is reviewed in order to make realistic approximations to the kinetic parameters which might be expected for the monolith converter using either base metal oxide or platinum catalysts.

The base metal oxidation of carbon monoxide is a first-order reaction in carbon monixide and independent of oxygen for oxygen concentrations greater than 2% (*3*). The base metal oxide rate expressions used in the calculations were estimated from those given by Kuo *et al.* (*3*), who used catalysts with base metal applied on the outer portion of alumina spheres. A rate expression was determined by assuming the reaction rate for the monolith converter would be the same based on the volume of active catalyst and by estimating the thickness of the catalytic layer on the monolith wall. Since the pre-exponential factor in the rate constant can vary according to catalyst deactivation, amount of active catalyst, *etc.*, we use the two rate expressions, B1 and B2, listed in Table I.

**Table I. Reaction Rate Expressions**

$$\text{B1:}\quad -r_{co} = 7.8 \times 10^5 \frac{Y_{co}}{T} \exp\left(-16000\ ^\circ\text{R}/T\right) \frac{\text{lb-mole}\ ^\circ\text{R}}{\text{min ft}^3}$$

$$\text{B2:}\quad -r_{co} = 3.9 \times 10^6 \frac{Y_{co}}{T} \exp\left(-16000\ ^\circ\text{R}/T\right) \frac{\text{lb-mole}\ ^\circ\text{R}}{\text{min ft}^3}$$

$$\text{P1:}\quad -r_{co} = Y_{o_2} Y_{co}/(0.5\, Y_{o_2} + 1.33\, Y_{co}^2 \exp\left(11000\ ^\circ\text{R}/T\right)) \frac{\text{lb-mole}}{\text{min ft}^3}$$

The oxidation of carbon monoxide on platinum is generally agreed to be a first-order reaction in oxygen and inversely proportional to carbon monoxide (*2, 7, 8*). The rate expression is negative order in carbon monoxide because of the strong adsorption of carbon monoxide on platinum. As pointed out by Schlatter *et al.* (*8*) the rate expression would not apply at low carbon monoxide concentrations. For the oxidation of carbon monoxide on platinum wire, Sklyarov *et al.* (*9*) report a rate expression similar to the Langmuir-Hinshelwood type. For the conditions of the monolith converter, their rate expression can be accurately approximated by:

$$r_{co} = Y_{o_2} Y_{co}/(k_1 Y_{o_2} + k_2 Y_{co}^2) \tag{1}$$

The first term in the denominator is important only at high temperatures and low carbon monoxide concentrations. Under other conditions the reaction would appear to be inversely proportional to carbon monoxide. A rate expression of the form of Equation 1 is used in the calculations. The activation energy in the constant $k_2$ was taken from Harned (*2*), although Harned assumed $k_1$ was zero. Sklyarov *et al.* (*9*) report a zero activation energy for

$k_1$, and this value is used here. The ratio of $k_1$ to $k_2$ was assumed to be the same as found by Sklyarov *et al.* (9) at 600°F. The magnitudes of the rate constants were estimated so that the platinum kinetics would give qualitatively the same comparison to the base metal kinetics as was observed by Schlatter *et al.* (8). The platinum rate expression, so determined, is designated P1 and listed in Table I.

Space limitations preclude a complete discussion of the justification of the assumptions. We therefore list the important assumptions and the available references.

1. The flow is laminar since Re $< 2000$ (*10*).

2. Except under conditions of very high flow rate, the velocity entry length is a small fraction of the converter length (*11*), and its effect on heat and mass transfer is small (*12*).

3. Axial diffusion in the fluid phase is negligible since Pe $> 50$ (*13*).

4. The transient response of the converter is controlled by the thermal response of the solid. All other time derivatives are set to zero (*1*).

5. Diffusion coupling can be neglected (*14, 15*).

6. The converter is adiabatic (*6*), and only a single cell is modeled. If the flow rate is different in adjacent cells, then a complete model must account for this flow distribution and repeat the single-cell calculations for each cell. This is beyond the scope of the present work.

7. The solid temperature at any axial position is uniform and equal to the fluid temperature at the fluid-solid interface.

8. Axial conduction in the solid is unimportant provided:

$$\left| r_h \frac{A^s}{A^f} k^s \frac{\partial^2 T^s}{\partial z^2} \right| \ll \left| \Delta H \, r_{co} \right|$$

9. Because the catalytic layer is very thin (*16*), internal diffusion effects in the catalytic layer are small and are included in the reaction rate expressions.

10. The concentration ratio of hydrogen to carbon monoxide is 1:3 everywhere in the reactor (*3, 7*).

11. The presence of hydrocarbons does not appreciably affect the conversion of carbon monoxide or the heat generated in the converter.

12. The mole fraction of oxygen is determined by stoichiometry.

Assumptions 9–12 are made because of a lack of sufficient information on the reaction kinetics. The calculations for which the inequality in assumption 8 does not hold are identified below. Although work is presently in progress to solve the problem relaxing assumptions 7 and 8 for typical irregular duct geometries, we solve the problem here for the case of a circular cross-section as an initial study. The governing equations are then:

$$\text{Model II: } 2r_h \, \mathrm{Pe}_h \, (1 - r^2) \frac{\partial T^f}{\partial z} = \frac{1}{r} \frac{\partial}{\partial r} \left( r \frac{\partial T^f}{\partial r} \right) \tag{2a}$$

$$2r_h \mathrm{Pe}_m \, (1 - r^2) \frac{\partial Y^f}{\partial z} = \frac{1}{r} \frac{\partial}{\partial r} \left( r \frac{\partial Y^f}{\partial r} \right) \tag{2b}$$

$$r_h \frac{A^s}{A^f} \frac{\rho^s C_p{}^s}{C_p{}^f} \frac{\partial T^s}{\partial t} = \frac{\Delta H}{C_p{}^f} r_{co} - \frac{2G}{\mathrm{Pe}_h} \frac{\partial T^f}{\partial r} \bigg|_{r=1} \tag{2c}$$

$$r_{co} = \frac{2G}{\mathrm{Pe}_m} \frac{\partial Y^f}{\partial r} \bigg|_{r=1} \tag{2d}$$

$$T^s = T^f \text{ at } r = 1; \; T^s = T_o{}^s(z) \text{ at } t = 0$$

$$T^f = T_o{}^f(t) \text{ and } Y^f = Y_o{}^f(t) \text{ at } z = 0$$

The resistance to heat and mass transfer is often modeled using heat and mass transfer coefficients. A model of this type can be derived by integrating Equation 2 across the cell cross-section and defining heat and mass transfer coefficients in the usual way. This approach results in the following governing equations:

$$\text{Model I: } r_h \, \text{Pe}_h \frac{\partial T^m}{\partial z} = \text{Nu} \, (T^s - T^m) \tag{3a}$$

$$r_h \, \text{Pe}_m \frac{\partial Y^m}{\partial z} = \text{Sh} \, (Y^s - Y^m) \tag{3b}$$

$$r_h \frac{A_s}{A^f} \frac{\rho^s C_p{}^s}{C_p{}^f} \frac{\partial T^s}{\partial t} = \frac{\Delta H}{C_p{}^f} r_{co} - \frac{G \, \text{Nu}}{\text{Pe}_h} (T^s - T^m) \tag{3c}$$

$$r_{co} = - \frac{G \, \text{Sh}}{\text{Pe}_m} (Y^m - Y^s) \tag{3d}$$

$$T^m = T_o{}^f(t) \text{ and } Y^m = Y_o{}^f(t) \text{ at } z = 0$$

$$T^s = T_o{}^s(z) \text{ at } t = 0$$

In the calculations, constant values of Nu and Sh are assumed while these quantities can be calculated from the solution of model II by:

$$\text{Nu} = 2 \frac{\partial T^f}{\partial r} \bigg|_{r=1} / (T^s - T^m) \tag{4}$$

The Sherwood number is defined analogously. If the quantities Nu and Sh used in model I are calculated from the solution of model II by using Equation 4, the two models will give an exact correspondence.

**Solution Method.** The model I equations may be solved in a straightforward manner. We use the improved Euler method in time and either the improved Euler method or the trapezoidal rule in the axial direction. At a given time the equations are solved in the axial direction, and the right side of Equation 3c is determined. This information is then used to step forward in time. Equation 3d and Equation 3c for steady-state calculations are solved analytically when linear, and by using the Newton-Raphson method when they are nonlinear.

For model II the orthogonal collocation method (*17*) is used. Using this method the radial Laplacian operators in Equations 2a and 2b are replaced by matrix operators, and the equations are then reduced to a set of nonlinear first-order differential equations. Unfortunately, the resulting set of ordinary differential equations tend to be stiff, and a small step size would be required if an explicit integration scheme were to be used. An implicit scheme would allow a larger step size but would require the solution of a set of nonlinear algebraic equations at each position step. For these reasons an efficient solution algorithm was devised, which utilizes the results of two similar Graetz problems. The problems of flow with (1) specified wall temperature and (2) specified wall flux were solved as eigenvalue problems. The solution to the two eigenvalue problems can be expressed in terms of integrals involving the wall temperature and the wall flux, respectively (*18*). By using interpolating polynomials to approximate these quantities in model II, the equations could be solved very efficiently. Another advantage of this solution algorithm is that the same computer program can be used to solve the problem in different

geometries, provided assumption 7 above is justified. To solve the problem for other geometries all that is necessary is to solve the analogous eigenvalue problem appropriate to the geometry of interest.

By this method the problem reduces to one of solving (*19*):

$$Y^m(z, t) = Y_o^t(t) + \frac{1}{r_h G}\int_o^z r_{co}\,[Y^s(\tau, t),\ T^s(\tau, t)]\,d\tau \tag{5}$$

$$Y^s(z, t) = Y^m(z, t) + r_{co}\,[Y^s(z, t),\ T^s(z, t)]\ \mathrm{Pe}_m/(2G\,A_{N+1,N+1})$$

$$+ \sum_{k=1}^{N-1}\left(\frac{Q_k}{4r_h G}\right)\int_o^z \exp\left[\frac{\lambda_k(z-\tau)}{2r_h\,\mathrm{Pe}_m}\right] r_{co}\,[Y^s(\tau, t),\ T^s(\tau, t)]\,d\tau$$

$$T^m(z, t) = T_o^t(t) + \sum_{k=1}^{N}\left(\frac{Q'_k}{2r_h\,\mathrm{Pe}_h}\right)\int_o^z \exp\left[\frac{\lambda'_k(z-\tau)}{2r_h\,\mathrm{Pe}_h}\right][T^s(\tau, t) - T_o^t(t)]d\tau$$

$$\left.\frac{\partial T^t}{\partial r}\right|_{r=1} = \frac{1}{2}\,r_h\,\mathrm{Pe}_h\,\frac{\partial T^m}{\partial z}\,(z, t) \tag{6}$$

$$= \sum_{k=1}^{N}\left(\frac{Q'_k}{2r_h\,\mathrm{Pe}_h}\right)\left(\frac{\lambda'_k}{2r_h\,\mathrm{Pe}_h}\right)\int_o^z \exp\left[\frac{\lambda'_k(z-\tau)}{2r_h\,\mathrm{Pe}_h}\right][T^s(\tau, t) - T_o^t(t)]d\tau$$

$$+ [T^s(z, t) - T_o^t(t)]\sum_{k=1}^{N}\frac{Q_k'}{2r_h\,\mathrm{Pe}_h}$$

The $Q_k$ and $\lambda_k$ are the coefficients and eigenvalues from the flux specified problem, and $Q'_k$ and $\lambda'_k$ are the analogous quantities from the wall temperature specified problem. Equations 5 and 6 together with 2c constitute model II. For steady-state conditions, Equations 2a and 2c become analogous to 2b and 2d, and then an equation of the form of Equation 5 is used for temperature. The problems are discretized in the axial direction by the use of interpolating polynomials. For Equation 5 we use polynomials of the form:

$$r_{co}(z) \simeq r_{co}(z_j, t)\,(1 - X^2) + \left.\frac{\partial r_{co}}{\partial z}\right|_{z_j,\,t}\Delta z(X - X^2) + r_{co}(z_{j+1}, t)\,X^2 \tag{7}$$

where $X = (z - z_j)/\Delta z$. For Equation 6 Lagrange interpolation is used. The interpolating polynomials are substituted into Equations 5 and 6, and the integration is performed. Since Equation 7 is implicit, this procedure resulted in one or two algebraic equations for transient and steady calculations, respectively, which must be solved at each axial step. This is accomplished analytically when the equations are linear or by Newton-Raphson iteration when they are nonlinear. For transient calculations the improved Euler method is used to integrate Equation 2.

### *Calculated Results*

Calculations have been performed for the two models by using the rate expressions in Table I. The parameter values common to all of the calculations are listed after the appropriate symbol in the Nomenclature section.

The model I equations are the same as those studied by Lui and Amundson (*20*) and can exhibit multiple solutions for some parameter values. The

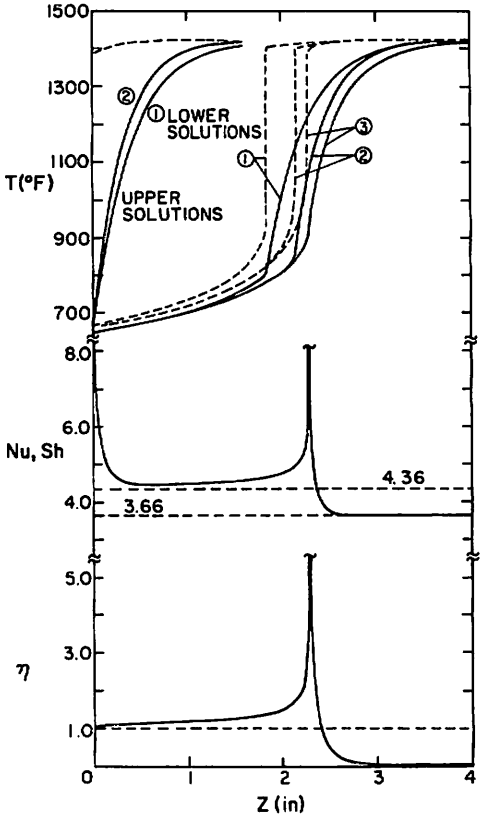


*Figure 1. Typical steady-state calculation using Pt (platinum) catalyst: – – – T′; —— T‴; F = 28.5 SCFM; $T_o' = 650°F$; $Y_o' = 0.04$; 1: model I, Nu = Sh = 3.5; 2: model I, Nu = Sh = 4.5; 3: model II*

analysis of Lui and Amundson can be applied directly to determine the parameter values for which multiple solutions can occur. Model I predicts multiple solutions to occur at high carbon monoxide concentrations with base metal catalyst, while with platinum catalyst they are predicted to occur over a wide range of conditions. Model II predicts that these multiple solutions cannot occur, and this result has been proved theoretically (*19*).

The calculations for typical cases using the two models and the three rate expressions are illustrated in Figures 1, 2, and 3. The asymptotic values of Nu and Sh, 3.66 for constant wall temperature and 4.36 for constant flux or linear wall temperature, are shown on the figures for reference. For cases when model I predicts multiple solutions the highest and lowest possible solutions are illustrated. The lower solution is typical of a situation when the converter is heated from an initial low temperature, while the higher solution results when the converter is cooled from some initial high temperature. For intermediate initial temperatures the final steady state may lie between those

shown. Such results are illustrated by Lui and Amundson (*20*) and have been confirmed for these kinetics by transient calculations using model I. Model II predicts only the one solution shown.

It is of particular interest that the solution for model II corresponds more closely to the lower solution of model I. Even if the lower solution of model I is chosen, model II predicts that the reaction will light off at a point further downstream than predicted by model I. Thus, model I always gives an optimistic prediction for the converter. These results can best be explained by observing the changes in the Nusselt number and effectiveness factor with position. The effectiveness factor is defined here as the reaction rate at the wall conditions divided by the reaction rate at the mixing cup fluid conditions. If mass and heat transfer were infinitely fast, then the effectiveness factor would always be unity. By observing the changes in these quantities, as illustrated in Figures 1, 2, 3, and 4, one can characterize the reactor in the following manner:

1. An initial entry length—In this region the Nusselt number decreases from an initial value of infinity in much the same manner as in a heat transfer problem.

2. A reaction limited region—In this region the effectiveness factor is near unity, and the conversion is limited by a low reaction rate.

3. A reaction zone—The reaction lights off, and the effectiveness factor and Nusselt number rise sharply.

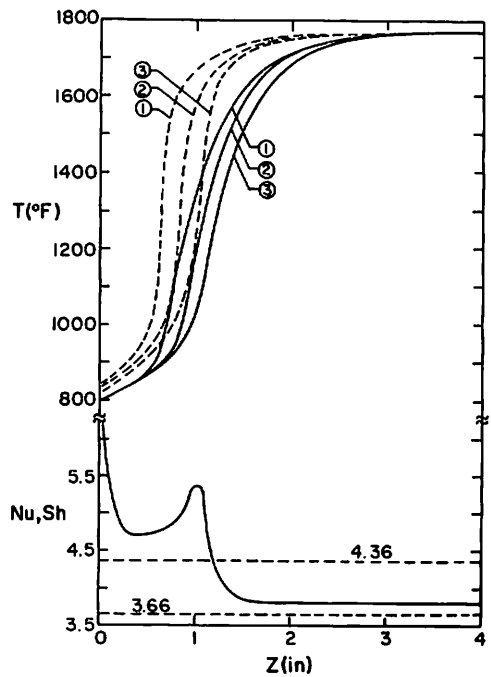


*Figure 2. Typical steady-state calculation using B1 (base metal) catalyst: - - - $T^s$; —— $T^m$; F = 28.5 SCFM; $T_o' = 800°F$; $Y_o' = 0.05$; 1: model I, Nu = Sh = 3.5; 2: model I, Nu = Sh = 4.2; 3: model II*

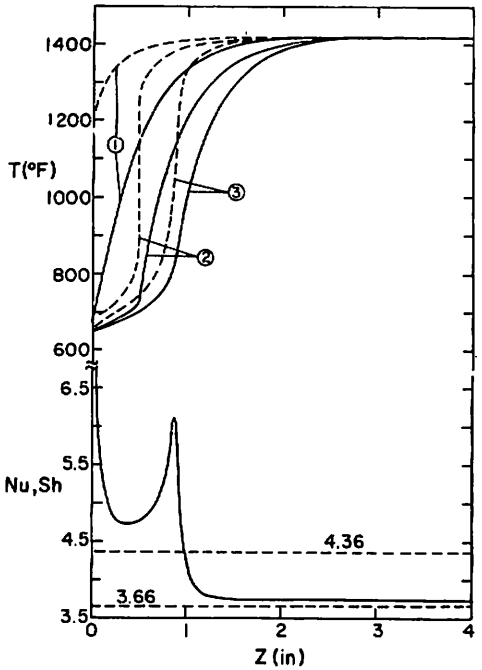


*Figure 3: Typical steady-state calculation using B2 (base metal) catalyst: - - - T′; —— T″; F = 28.5 SCFM; T.′ = 650°F; Y.′ = 0.04; 1: model I, Nu = Sh = 3.5; upper solution; 2: lower solution of 1; 3: model II*

4. A second entry length—After the reaction zone the Nusselt number goes through a second transition similar to the initial entry length.

5. A mass and heat transfer limited region—After the reaction zone the conversion is limited by the rate at which carbon monoxide can be transferred to the converter wall.

The discrepancy between model I and model II arises from the failure of model I to predict accurately the phenomena occurring in the reaction zone. In model I the Nusselt and Sherwood numbers are assumed to remain at their asymptotic values. Therefore, one must solve model II to accurately determine the transport rates in the converter.

Using the inequality in assumption 8, we determine the importance of axial conduction in the converter wall. For conditions when model I predicts multiple solutions there is a discontinuity in the wall temperature, so axial conduction would always be important in these cases. Indeed, Eigenberger (*21*) has shown that when axial conduction in the solid phase is included in model I, the infinite multiplicity of steady states reduces to two or three depending on the axial boundary conditions. Using model II, there is no discontinuity in wall temperature. In Figures 2 and 3 axial conduction is relatively unimportant, while in Figure 1 the ratio of axial conduction to reaction is 1.9 at $z = 2.28$ inches, using a value of $k^s = 0.83$ Btu/hr ft °F. Since the reaction on platinum catalyst is strongly autocatalytic, the wall temperature rises rapidly in the reaction zone and axial conduction is important.

Morgan *et al.* (*6*) have discussed a phenomenon called emission breakthrough. Even though the reactor is fully warmed up some carbon monoxide can pass through the converter unreacted. This phenomenon can occur when there is insufficent oxygen for complete conversion, or when the flow rate through the converter is high. An example of this type of situation is shown in Figure 4. Under conditions when the reaction rate is large, the first four regions in the reactor, discussed above, combine into one, and the conversion is limited by mass transfer considerations. In Figure 4 the amount of carbon monoxide present at the outlet is 2.5% of that at the inlet even though the reaction lights off near the inlet of the converter. The discrepancy between model I and model II has particular significance for this situation, because model I always gives an optimistic prediction. As suggested by Morgan *et al.* (*6*), this problem can be reduced by increasing the converter length. Morgan *et al.* (*6*) also suggest that a converter geometry with good mass transfer be used. As stated above, in the limiting case of infinite transfer rates the effectiveness factor would be unity throughout the reactor. High mass transfer

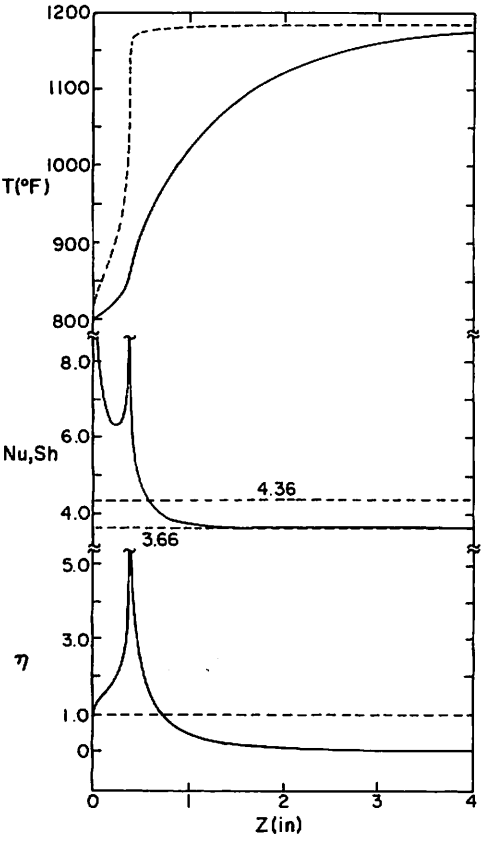


*Figure 4. An example of emission breakthrough predicted by model II: --- T′; —— T‴; P1 catalyst; F = 80 SCFM; $T_o' = 800°F$; $Y_o' = 0.02$*

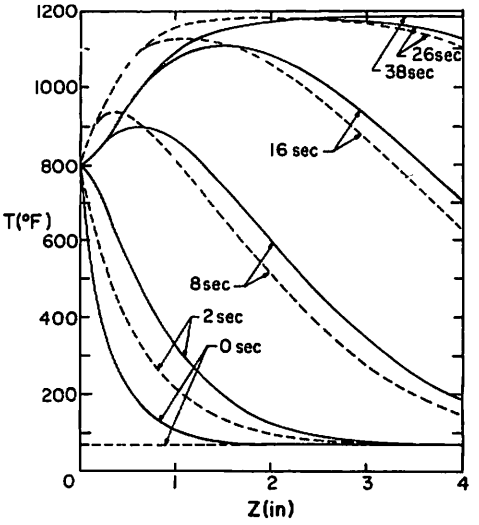


*Figure 5. A warmup transient calculation using model II: --- $T^s$; —— $T^m$; B2 catalyst; F = 28.5 SCFM; $T_o' = 800°F$; $Y_o' = 0.02$; $T_o' = 70°F$*

rates are beneficial in the transfer limited region of the reactor, but detrimental in the reaction limited region. This effect is suggested, too, by the calculations using model I in Figures 1 and 2. A converter geometry with good transfer characteristics would probably be advantageous only in the case when the converter is purely mass and heat transfer limited.

Transient calculations have also been performed using the models. A calculation of converter warmup is illustrated in Figures 5 and 6. The transient response of the converter is indeed very fast. For this particular case, the conversion is essentially complete for all times greater than 15 sec. Model I gives a conservative prediction in this transient case because relatively low values of the Nusselt and Sherwood numbers were used. The variations of Sh and Nu in Figure 6 are interesting. When the mixing cup temperature and wall temperature intersect, the Nusselt number decreases to minus infinity and then jumps to plus infinity. At small times Sh decreases to low values caused by the rapidly decreasing reaction rate.

As stated above, during certain critical driving modes high temperatures can occur in the monolith converter. The following example is typical of what might happen when the automobile is cruising at highway speeds and then decelerates over some time interval to a lower speed. For this situation we use the following parameters:

$$F = 80 \text{ SCFM}, \; Y'_o = 0.01, \; t < 0$$

$$F = 28.5 \text{ SCFM}, \; Y'_o = 0.04 \; t > 0$$

The results using P1 catalyst are shown in Figure 7, and for B2 catalyst in Figure 8. The wall temperature during the transient exceeds the adiabatic temperature, which is the maximum wall temperature which can occur at the end of the transient. This phenomenon has been observed by Lui and Amund-

son (*20*) for model I; however, for these conditions model I does not exceed the adiabatic temperature while model II predicts that the adiabatic temperature is exceeded by 100°F. Although the temperatures here would not cause damage to the converter, if the inlet temperature or concentration had been higher, this overshoot phenomenon could cause damage to the converter. Figure 8 shows that with B2 catalyst the overshoot is less severe (25°F). These results would be affected by axial conduction. It will be very interesting to see if a similar phenomenon occurs when axial conduction is included in the converter model.

### *Accuracy and Computation Time*

The validity of the results depend, of course, on the accuracy of the computation scheme. Other computations suggest that the results are accurate to within a few degrees. The order of approximation required depended strongly on the particular case studied. As stated above, model II can only have a single

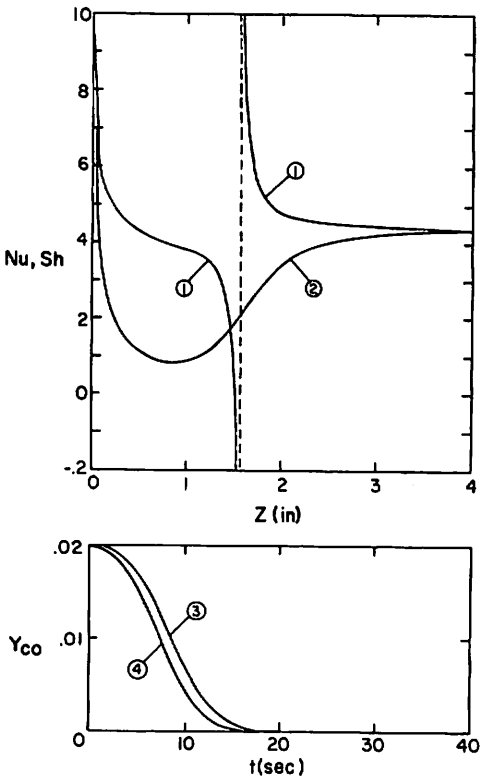


*Figure 6. For the transient shown in Figure 5: Nu and Sh distributions during the transient; 1: Nu at* t = *16 sec; 2: Sh at* t = *2 sec; and outlet carbon monoxide mole fractions predicted by the two models; 3: outlet mole fraction, model I, Nu = Sh = 3.5; 4: outlet mole fraction, model II*

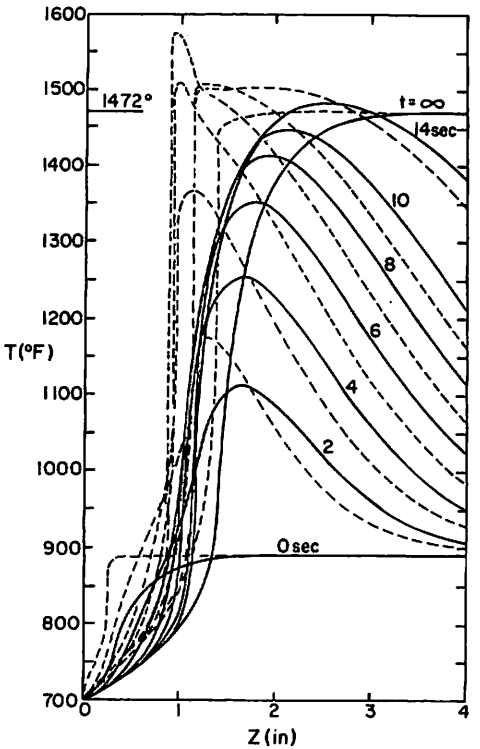


*Figure 7. Transient resulting from vehicle deceleration from cruising speed using P1 (platinum) catalyst: --- $T^s$; —— $T^m$; F = 28.5 SCFM; $T_o' = 700°F$; $Y_o' = 0.04$; $T_o'(z)$ from steady state with F = 80 SCFM, $T_o' = 700°F$, $Y_o' = 0.01$; model II – transient; 1472°F = adiabatic temperature at t = ∞*

steady state; however, the model equations were solved approximately, and it was sometimes necessary to use a very accurate approximation to obtain only a single solution. The results in Figure 1 required 2000 axial steps and five radial collocation points, resulting in a computation time of 10 sec. Computation times are for a CDC 6400 computer. Accurate results for the cases in Figures 2 and 3 could be obtained using three radial collocation points and 200 axial steps (0.4 sec).

During transient calculations a variable time step size was used, while in the axial direction the grid spacing was fixed. The step size was controlled by requiring the correction in the improved Euler method to remain within specified limits. This method of step size control worked well. The transient calculations in Figures 5 and 6 used 160 axial steps and four radial collocation points and required 50 sec of computation. The most extreme case, Figure 7, utilized 1000 axial grid points and four collocation points and required 900 sec of computer time. The strongly autocatalytic rate expression for platinum catalyst required accurate approximations and resulted in large computation times.

### *Conclusions*

The distribution of mass and energy in the cross-section of the monolith cells is important and must be included in the converter model. Under conditions when the wall temperature rises sharply axial conduction in the converter wall must be included in the reactor model, although it was not included in this preliminary study. A solution algorithm which utilizes the results from the analogous eigenvalue problem allows one to solve the problem efficiently, and for different geometries. The orthogonal collocation method is an efficient method of solving the eigenvalue problems.

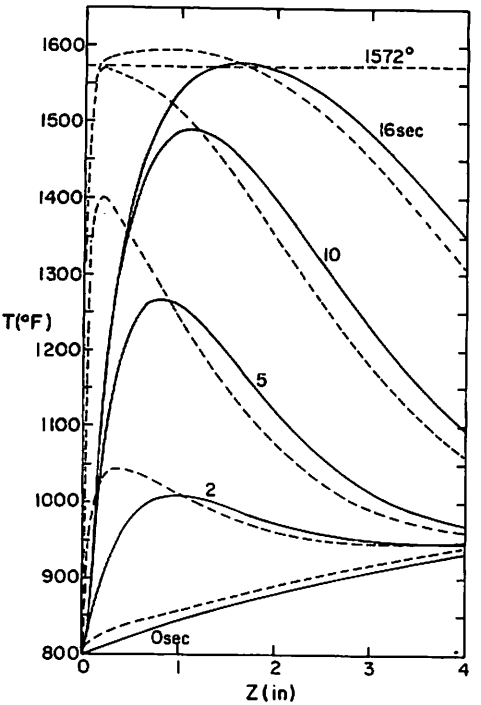


*Figure 8. Transient resulting from vehicle deceleration from cruising speed using B2 (base metal) catalyst: - - - T'; —— T'; F = 28.5 SCFM; $T_o' = 800°F$; $Y_o' = 0.04$; $T_o'(z)$ from steady state with F = 80 SCFM, $T_o' = 800°F$, $Y_o' = 0.01$; model II – transient; 1572°F = adiabatic temperature at t = ∞*

Although axial conduction in the converter wall is important in some of the calculations, the calculations suggest that the wall temperature during some transients can significantly exceed the adiabatic temperature. The calculations also suggest that a converter cell geometry with very good mass and heat transfer characteristics may not always be preferable to a geometry with poor transfer characteristics.

*Acknowledgment*

The authors thank Engelhard Industries for supplying a noncatalytic PTX-4 converter for study. This research was supported by the National Science Foundation under Grant No. GK-12517 and by the donors of the Petroleum Research Fund, administered by the American Chemical Society under grant PRF 5965-AC7.

*Nomenclature*

| | |
|---|---|
| $A^f$ | frontal area of fluid, 5.54 inches$^2$ |
| $A^s$ | frontal area of solid, 2.77 inches$^2$ |
| $A_{N+1,N+1}$ | element of orthogonal collocation discretization matrix |
| $C_p{}^f$ | molar heat capacity of fluid, 7.5 Btu/lb-mole °F |
| $C_p{}^s$ | solid heat capacity, 0.2 Btu/lb °F |
| $F$ | flow rate through converter, SCFM |
| $G$ | molar velocity, 0.0704 F lb-mole/min ft$^2$ |
| $\Delta H$ | heat of reaction, $-145{,}000$ Btu/(lb-mole CO + $\frac{1}{3}$ lb-mole $H_2$) |
| $k_1, k_2$ | rate constants |
| $k^s$ | thermal conductivity of solid, 0.83 Btu/hr ft °F |
| $N$ | number of interior collocation points |
| Nu | Nusselt number |
| $Pe_h$ | Peclet number for heat, 0.7 Re |
| $Pe_m$ | Peclet number for mass, 0.7 Re |
| $Q_k$ | coefficients for flux specified eigenvalue problem |
| $Q'_k$ | coefficients for wall temperature specified eigenvalue problem |
| $r$ | radial coordinate |
| $r_{co}$ | rate of carbon monoxide generation, lb-mole/min ft$^2$ |
| $r_h$ | hydraulic radius, duct area/duct perimeter, 0.012 inch |
| Re | Reynolds number, 5.62 F |
| Sh | Sherwood number |
| $t$ | time, sec |
| $T$ | temperature, °R |
| $Y, Y_{co}$ | mole fraction of carbon monoxide |
| $Y_{o_2}$ | mole fraction of oxygen, $\frac{2}{3}(0.03 + Y_{co})$ |
| $z$ | axial coordinate, inches |
| $z_j$ | axial grid point, $j\Delta z$, inches |
| $\Delta z$ | axial step size, inches |

**Greek Letters**

| | |
|---|---|
| $\eta$ | effectiveness factor |
| $\lambda_k$ | eigenvalues for flux specified eigenvalue problem |
| $\lambda'_k$ | eigenvalues for wall temperature specified eigenvalue problem |
| $\rho^s$ | solid density, 100 lb/ft$^3$ |

**Subscripts and Superscripts**

| | |
|---|---|
| f | value for fluid |
| m | bulk mixed fluid value |
| o | inlet or initial value |
| s | value for solid |

(The dimensionless quantities are nondimensionalized using the hydraulic diameter, 4 $r_h$.)

### *Literature Cited*


1. Ferguson, N. B., Finlayson, B. A., *AIChE, Nat. Meetg.*, Nov. 11-15, 1973, paper 40c.
2. Harned, J. L., *SAE, Meetg.*, 1972, paper 720520.
3. Kuo, J. C. W., Morgan, C. R., Lassen, H. G., *SAE, Meetg.*, 1971, paper 710289.
4. Wei, J., *Chem. Eng. Prog. Monograph Ser.* (1969) No. 6, **65.**
5. Kuo, J. C. W., private communication, 1973.
6. Morgan, C. R., Carlson, D. W., Voltz, S. E., *SAE, Meetg.*, 1973, paper 730569.
7. Langmuir, I., *Trans. Faraday Soc.* (1922) **17,** 621.
8. Schlatter, J. C., Klimisch, R. L., Taylor, K. C., *Science* (1973) **179,** 798.
9. Sklyarov, A. V., Tret'yakov, I. I., Shub, B. R., Roginskii, S. Z., *Doklady Akademii Nauk SSSR* (1969) **189,** 1302.
10. Knudsen, J. G., Katz, D. L., "Fluid Dynamics and Heat Transfer," McGraw-Hill, 1958, p. 105.
11. Fleming, D. P., Sparrow, E. M., *Trans. Amer. Soc. Mech. Eng. Ser. C* (1969) **91,** 345.
12. Monohar, R., *Int. J. Heat Mass Transfer* (1969) **12,** 15.
13. Hennecke, D. K., *Wärme-und Stoffürbertragung* (1968) **1,** 177.
14. Bird, R. B., Stewart, W. E., Lightfoot, E. N., "Transport Phenomena," John Wiley & Sons, Inc., 1960, p. 571.
15. Soloman, R. L., Hudson, J. L., *AIChE J.* (1971) **17,** 371.
16. Harned, J. L., Montgomery, D. L., *SAE, Meetg.*, 1973, paper 730561.
17. Finlayson, B. A., "The Method of Weighted Residuals and Variational Principles," Academic Press, New York, 1972.
18. Franklin, J. N., "Matrix Theory," Prentice-Hall, Englewood Cliffs, 1968, p. 57.
19. Young, L. C., Ph.D. Thesis, University of Washington, Seattle, Wash., August, 1974 (est.).
20. Lui, S., Amundson, N. R., *Ind. Eng. Chem., Fund.* (1962) **1,** 200.
21. Eigenberger, G., *Chem. Eng. Sci.* (1972) **27,** 1909, 1917.


RECEIVED January 2, 1974.